

EFFECT OF OBSTACLE IN RIVER ON THE HEAT DISSIPATION OF HOT WATER INJECTION

Ayser M. Fleh
Mech. Engr. Dept.
College of Eng. /Univcrity of Baghdad
Baghdad-Iraq

ABSTRACT

Numerical analysis of the cooling process of hot water discharge from a steam power plant into a river has been carried out in the present study. A mathematical model describing the flow field and temperature distribution induced in the river as a result of the cooling process is made based upon the assumptions of steady state, two-dimensional, turbulent flow, in the horizontal plane. The governing equations are the continuity, the momentum, the (K-ε) turbulence model and the energy equation. A proper initial and boundary condition are specified to be used in the solution of the governing equations. A numerical solution of the governing equations is made by using the control volume approach, with non-staggered grid technique and modified SIMPLE algorithm. The numerical solution is capable of calculating the velocity and temperature distributions of the calculation domain. The numerical results show that the developed algorithm is capable of calculating the flow field, properly and accurately. Results are obtained for ten cases of configuration, constant aspect ratio and weather conditions for Baghdad. The results show that the injection velocity effect on the temperature distribution and stream line , the exist of obstacle and its distance from the injection zone but the increase in injection temperature cause a small effect on temperature distribution and stream line.

الخلاصة

تقدم هذه الدراسة تحليلاً عددياً لعملية تبريد الماء الساخن المتدفق من مكثفات محطات الطاقة الكهربائية إلى النهر. فقد تم وضع نموذجاً رياضياً يصف طبيعة الجريان والتوزيع الحراري الحاصل في النهر نتيجة لعملية التبريد تلك، وقد اعتمد هذا النموذج على فرضيات منها حالة الاستقرار، ثنائي البعد، الجريان مضطرب في المستوى الأفقي. يتضمن النموذج الرياضي اشتقاق المعادلات التفاضلية الجزئية للمسألة، والتي هي معادلات الاستمرارية، الزخم، معادلتى نموذج (K-ε) للاضطراب ومعادلة الطاقة. بالإضافة إلى ذلك، تم تعريف ظروف ابتدائية وحدية مناسبة لاستخدامها في حل المعادلات. تم حل المعادلات عددياً باستخدام تقنية الحجم المحكوم مع شبكة غير مزحفة وطريقة (SIMPEL) المعدلة. للحل العددي القابلية على حساب توزيعات السرعة ودرجات الحرارة. أظهرت النتائج العددية ان النموذج العددي الذي تم التوصل إليه له القابلية على حساب الجريان بصورة مناسبة ودقيقة ولقيمة ثابتة (نسبة طول النهر الى عرضها aspect ratio) وللظروف الجوية لمدينة بغداد. ولقد أظهرت النتائج مياه النهر القريب من منطقة التدفق تتأثر بزيادة سرعة التدفق، زيادة درجة الحرارة، قرب وبعد الجسم العائق وكذلك وجود العائق وتتاثر قليلاً بزيادة درجة الحرارة.

KEY WORDS

Obstacle in River, Velocity and Temperature Field, Steady state, two-dimension, Horizontal Plane, Constant aspect ratio.

INTRODUCTION

Cooling water for steam power plants is in most cases supplied from rivers, lakes, artificial water ponds or cooling tower. Thermal pollution of water is considered a water temperature rise due to artificial reasons. Basically the rise at temperature may be observed naturally and be caused by many natural reasons. The degree of heating expressed in temperature may vary from several degrees (e.g. run-of waters from area exposed for solar radiation) up to extremely high degree (e.g. when lava flows into the ocean). If artificial reasons are concerned, the main impact associated to water temperature rise is generated by industry. Water with its high heat capacity is considered as good cooling medium in industry. It is estimated that electric generating plants are the main source of thermal pollution in rivers and water reservoirs (**H.Inhaber 2005**). Furthermore, nuclear power plants reject all heat to the cooling water system, and emit 50% more heat than heat than a fossil fuel stations (with a similar amount of produced electricity, (**Joyce and Port 1999**)). Nowadays the opinion predominates that thermal pollution due to hot waste water badly affects aquatic environment. Thermal shock can harm fish and organisms, and thermal enrichment, in spite of several positive aspects, (e.g. melting ice snow or warm water use in green houses) may be finally harmful for biocenosis (lack of dissolved oxygen). The main advantages of river are simplicity, low maintenance, and ability to operate for extended periods without the need for make-up water and, the low power requirements, as the only mechanical equipment needed are pumps for occasional addition of make up water. Circulating water pumps are of course needed by river, as by all other systems. Hot water from the condenser is simply dumped into a river and left to cool. Cool water from the river is returned to the condenser. The river performance is important to the efficiency of the power plant itself because a condenser operating at a lower temperature results in more turbine work and operating at a lower temperature. Results in more turbine work and cycle efficiency, and less heat rejection. It was found that a difference of (5 C) in the natural temperature of a cooling river between winter and summer reduces the thermal efficiency of power plant by approximately (1%) in summer (**A. Zukauskas 1976**). The present work deals with velocity and temperature distribution in a river as a means to evaluate heat dissipation. For such analysis values are needed for eddy viscosity and diffusivity. Literature survey indicates that value for these parameters used by other workers range between ($2.5 * 10^{-4}$ to $0.1 * 10^{-2} m^2/s$).

The problem was investigated in literatures with different a approaches. (**American Society of Civil Engineering.1988**) the turbulence models regarding surface water flow. (**Nogano and Tagawa. 1990**) made an improvement of the K- ϵ model in conjunction with an accurate prediction of the near-wall limiting behavior of turbulence and the final period of the decaylaw of free turbulence. This improved $k - \epsilon$ model has been extended to predict the effects of adverse pressure gradients on shear layers, which most previously proposed models failed to do correctly. (**Anis AL-Layla and Hasan Al-Rizzo1990**), describes the development and calibration of a mathematical model for the Tigris River downstream of AL Mosul. The river stretch studied is 75km long extending from the Al Mosul Dam to Mosul city. The field work was conducted during the period from July to September 1986. Water samples were collected bimonthly from specified sampling points. (**Michael Manga and James W.Kirchner 2004**), circulating groundwater transports heat. If groundwater flow velocities are sufficiently high, most of the subsurface heat transport can occur by advection. This is the case, for example, in the Cascades volcanic arc where much of the background geothermal heat is transported adjectively and (**Andrzej Pozlewicz2006**), Special attention is paid to electric generating plants where cooling water are mixed with a river. The study area covers the lower part of Odra River, near Szczecin, Poland, where the main thermal pollution sources are power plants and coal combustion is used in energy production. The river

flows through Szczecin in two beds linked by several canals, lake and creates a complex hydraulic system. The mean discharge flow rate in Odra River is 500-600 m^3/s , and the mean velocity 0.3-0.5 m/s.

MATHEMATICAL MODELING

The usual system of Cartesian coordinates will be adapted, the x-axis being along the wall, and the y-axis being at right angle to it. Injection will be accounted for by prescribing non-zero normal velocity component (V_w) at the wall. In the case of and $V_w > 0$ will be used for injection, see **Fig (1)**. Two-dimensional flow and heat transfer ($w = 0, \frac{\partial}{\partial z} = 0$), Uniform suction or injection ($V_w = \text{constant}$).

Negligible axial diffusion ($\frac{\partial^2}{\partial x^2} = 0$).

According to the previously mentioned assumptions, the governing conservation and constitution laws will be presented here in terms of the geometry and coordinates system of **Fig (1)**. these are the continuity, the momentum, the (\mathbf{k} - ϵ) turbulence model and the energy equations.

Continuity Equation

$$\frac{\partial}{\partial x}(\rho u) + \frac{\partial}{\partial y}(\rho v) = 0 \quad (1)$$

Momentum Equation in X-Direction;

$$\left(u \frac{\partial u}{\partial x} + v \frac{\partial u}{\partial y} \right) = -\frac{\partial P}{\partial x} + \frac{\partial}{\partial y} \left(\mu \frac{\partial u}{\partial y} \right) + \frac{\partial}{\partial y} \left(\mu_t \frac{\partial u}{\partial y} \right) \quad (2)$$

Momentum Equation in Y-Direction;

$$\left(u \frac{\partial v}{\partial x} + v \frac{\partial v}{\partial y} \right) = -\frac{\partial P}{\partial y} + \frac{\partial}{\partial y} \left(\mu \frac{\partial v}{\partial y} \right) + \frac{\partial}{\partial y} \left(\mu_t \frac{\partial v}{\partial y} \right) \quad (3)$$

The standard form of (K- ϵ) model is as follows:-

Turbulence Kinetic Energy Equation;

$$\left(u \frac{\partial \kappa}{\partial x} + v \frac{\partial \kappa}{\partial y} \right) = \frac{\partial}{\partial y} \left(\frac{\mu_t}{\sigma \kappa} \frac{\partial \kappa}{\partial y} \right) + \mu_t \left(\frac{\partial u}{\partial y} \right)^2 - \rho \epsilon \quad (4)$$

And dissipation of turbulence kinetic energy equation;

$$\left(u \frac{\partial \epsilon}{\partial x} + v \frac{\partial \epsilon}{\partial y} \right) = \frac{\partial}{\partial y} \left(\frac{\mu_t}{\sigma \epsilon} \frac{\partial \epsilon}{\partial y} \right) + \mu_t c_{\epsilon_1} \frac{\epsilon}{\kappa} \left(\frac{\partial u}{\partial y} \right)^2 - c_{\epsilon_2} \rho \frac{\epsilon^2}{\kappa} \quad (5)$$

According to the high Reynolds number ($\kappa - \varepsilon$) turbulence model the turbulent viscosity μ_t is related to the turbulent kinetic energy (κ) and to the dissipation of turbulent kinetic energy (ε) through the expression

$$\mu_t = c_\mu \rho \frac{\kappa^2}{\varepsilon} \quad (6)$$

The effective viscosity (μ_{eff}) is related to the turbulent viscosity (μ_t) and to the molecular viscosity (μ) through the relation :-

$$\mu_{eff} = \mu + \mu_t \quad (7)$$

In the above equations, ($c_\mu, c_{\varepsilon_1}, c_{\varepsilon_2}, \sigma_k, \sigma_\varepsilon$) are constants at high Reynolds number and the model constant $c_\mu, c_{\varepsilon_1}, c_{\varepsilon_2}, \sigma_k, \sigma_\varepsilon$ are set to $c_\mu = 0.09, c_{\varepsilon_1} = 1.44, c_{\varepsilon_2} = 1.92$. Usually, the constant σ_k and σ_ε are assigned to $\sigma_k = 1.0$ and $\sigma_\varepsilon = 1.3$ (Lauder and Spalding 1974)

Energy Equation;

$$\rho cp \left(u \frac{\partial T}{\partial x} + v \frac{\partial T}{\partial y} \right) = \frac{\partial}{\partial y} \left(k \frac{\partial T}{\partial y} \right) + \frac{\partial}{\partial y} \left(k_t \frac{\partial T}{\partial Y} \right) \quad (8)$$

Where;

$$k_t = \frac{\mu_t cp}{Pr_t} \quad (9)$$

For the evaluation of turbulent kinetic energy and dissipation at turbulent Kinetic energy, it is sufficed to fix their values at the near wall node (P) according to the following formula:-

$$\kappa_P = \frac{\tau_\omega}{\rho c_\mu^{1/2}} \quad (10)$$

$$\varepsilon_P = \frac{c_\mu^{3/4}}{V_K y_P} \kappa_P^{3/2} \quad (11)$$

$$y^+ = \frac{\rho y_p c_\mu^{1/4} k_p^{1/2}}{\mu_t} \quad (12)$$

Where (y_p) is the normal distance of the near wall node (p) to the solid surface. In the above formula, (k) is the Von Karman constant (0.4187) and (E) is an integration constant that depends on the roughness of the wall. For a smooth wall constant shear stress, (E) has a value of (9.793).

The initial and boundary conditions of problem are shown in **Fig (2)**. All the previously discussed differential equations can be conveniently presented in the general form.

$$\frac{\partial}{\partial x} (\rho u \phi) + \frac{\partial}{\partial y} (\rho v \phi) - \frac{\partial}{\partial y} \left[\Gamma_\phi \frac{\partial \phi}{\partial y} \right] = s_\phi \quad (13)$$

In the above equation, ϕ identifies the dependent variables, Γ_ϕ is the appropriate exchange coefficient for the variable ϕ , and S_ϕ are the source term which includes both the sources of ϕ and any other terms which cannot find place on the left-hand side of **Eq. (13)**

The derived governing equations and the initial and boundary conditions in **Fig. (2)** will be solved numerically by using the control volume approach of **(Patanker1980)**. The finite difference method (F.D.M.) will be used, and the details of the numerical solution will be described in the next article.

NUMERICAL SOLUTION

The general form **Eq. (13)** may be written as;

$$\frac{\partial}{\partial x} \left[\rho u \phi - \Gamma_\phi \frac{d\phi}{dx} \right] + \frac{\partial}{\partial y} \left[\rho v \phi - \Gamma_\phi \frac{d\phi}{dy} \right] = S_\phi \quad (14)$$

By defining J as the total flux which consists of convection and diffusion fluxes, or

$$J_x = \rho u \phi - \Gamma \frac{\partial \phi}{\partial x} \quad (15)$$

$$J_y = \rho v \phi - \Gamma \frac{\partial \phi}{\partial y} \quad (16)$$

Where J_x and J_y are the total fluxes through faces normal to the x and y directions respectively with these definitions, **Eq. (14)** can be written

$$\frac{\partial J_x}{\partial x} + \frac{\partial J_y}{\partial y} = S_\phi \quad (17)$$

Eq. (17) was integrated by using the finite volume approach of **(Patanker 1980)**, see **Fig. (3)** The source term has been linearized, and the values at the control volume faces (e,w,n,s) are assumed to be found by linear interpolation (central difference) . The resulting final form of **Eq. (17)** becomes

$$\frac{(\rho_P \phi_P - \rho_P^\circ \phi_P^\circ) \Delta x \Delta y}{\Delta t} + J_e - J_w + J_n - J_s = (S_c + S_p \phi_P) \Delta x \Delta y \quad (18)$$

$$a_P \phi_P = a_E \phi_E + a_W \phi_W + a_N \phi_N + a_S \phi_S + b$$

$$a_E = D_e A(P_e) + \text{Max}[-F_e, 0]$$

$$a_W = D_w A(P_w) + \text{Max}[F_w, 0] \quad (19)$$

$$a_N = D_n A(P_n) + \text{Max}[-F_n, 0]$$

$$a_S = D_s A(P_s) + \text{Max}[F_s, 0]$$

$$a_P^\circ = \frac{\rho_P^\circ \Delta x \Delta y}{\Delta t} \quad b = S_c \Delta x \Delta y + a_P^\circ \phi_P^\circ \quad (20)$$

$$a_P = a_E + a_W + a_N + a_S + a_P^\circ - S_p \Delta x \Delta y \quad (21)$$

$$\begin{aligned}
 \phi_e &= \phi_E f_e + \phi_p [1 - f_e] \\
 \phi_w &= \phi_W f_w + \phi_p [1 - f_w] \\
 \phi_n &= \phi_N f_n + \phi_p [1 - f_n] \\
 \phi_s &= \phi_S f_s + \phi_p [1 - f_s]
 \end{aligned}
 \tag{22}$$

Generally

$$a_p \phi_p = \sum_{nb} a_{nb} \phi_{nb} + b \qquad nb = E, W, N, S \tag{23}$$

Where: b = Absolute part of the discredited equation

COMPUTER PROGRAMS

Computer programs are developed in FORTRAN 90 to perform the numerical solution formulated previously. The program consists of 3 main parts. The first is for grid generation. The second deals with solving the five non-linear, partial differential equations and the third deals with displaying the large quantity of results in a simplified form. In the first part of the program (**MESHGEN**), the mesh distribution of the model is generated. The resulting grid is stored in an external file and plotted on the screen for visual checking. In the second part (**MODEL**), the five non-linear, partial differential equations (u-velocity momentum equation, continuity equation, turbulent kinetic energy equation (K), turbulent energy dissipation equation (ε) and energy equation (T) are solved. The equations are solved in a sequential order after applying the appropriate boundary condition to each equation. In the third part (**PLOT**), the displaying of the large quantity of results in simplified standard windows graphics is made. This includes plotting the made, grid the velocity vectors and contour lines in **Fig.4**.

RESULTS AND DISCUSSION

The developed computational algorithm is tested for the take part in Tigris River 1000m long, 150m width and input river obstacle variable (dimensions, near river, further river) 5m long and 3m width. The obstacle near (+15m) and obstacle further (-15m) from injection. The Mach number was taken as (0.5), the free stream velocity (1m/s). Velocity injection equals to (0.1, 0.9m/s). The Reynolds number of the flow is (1×10^7) the temperature surface ($25\text{ }^\circ\text{C}$) with the free stream pressure and temperature (101325 pa) and ($25\text{ }^\circ\text{C}$) respectively. The Iraqi standard for thermal pollution according to environmental protection law (**Ministry of health directorate genera of human environment 1967**) is that' no hot water should be discharged into natural water resources on which its temperature is greater than ($35\text{ }^\circ\text{C}$) ", as well as another world wide limit at powre stations that thermal pollution should not exceed $3\text{ }^\circ\text{C}$ in the receiving water at mixing zone in case of river condition (**International atomic energy 1974**). The numerical results show that the developed algorithm is capable of calculating the flow field, properly and accurately. Taken as follow:-

Case No.1 present normal section without obstacle and without injection show the **Fig (1)**

Case No.2 river region with obstacle in the middle and without injection.

Case No.3 river region with obstacle in the middle and with injection (0.3 m/s, T-inj=308 K).

Case No.4 normal region without obstacle and with injection (0.3 m/s, T-inj=308 K).

CaseNo.5 without obstacle in river and increase injection velocity (0.9 m/s, constant - temperature injection).

CaseNo.6 obstacle in river and increase injection velocity (0.9 m/s, constant temperature - ---- injection.

CaseNo.7 obstacle in river, increase injection velocity and increase injection temperature ---
(0.9 m/s, $T_{inj}=313$ K).

CaseNo.8 obstacle in river, increase injection velocity and increase injection temperature ---
(0.9 m/s, $T_{inj}=318$ K).

Case No.9 same as 6, with obstacle closer to injection.

Case No.10 same as 6, with obstacle further to injection

The difference equations of this study were solved on a digital computer using **FORTTRAN 90** program and the mat lab program was used **MAT LAB** the isotherm and streamline contours.

The Flow Field

Case1: The first water body configuration that was considered in this work has a rectangle shape without obstacle and without injection. The numerical results of the stream function were drawn as equipotential lines giving the trend of the flow all over the river which is without obstacle as shown in **Fig. (5)**

For case2: **Fig. (6)** Shows the stream lines of the flow with obstacle and without injection. The streamlines were shown to be simple diffuse in obstacle region.

In case3 higher diffuse in streamlines compared with case 2 for a large portion of the obstacle is clear in **Fig. (7)** because of the existing of the injection. After the obstacle the stream lines were equipotential lines giving the trend of the flow.

Stream lines in case4 were diffuse clearly in a large portion of the river in the zone of injection without obstacle as in **Fig. (8)**.

In case 5 for higher injection velocity ($v \times 3$) compared with case 4 it is clear that the characteristics of the flow field is relatively similar to that in case 4 for the region far away from the injection zone as shown in **Fig. (9)**.

For case 6 which is as case 3 but with higher injection velocity ($v \times 3$), **Fig. (10)** Shows more diffusion in flow compared with **Fig. (7)**.

It is clear from **Fig. (11)** and **Fig. (12)** that the increase in injection temperature ($T_{inj} = 298^\circ$ K for case 6 and $T_{inj} = 343^\circ$ K for case 7) cause the flow to move longitudinally occupying the end of the region and a disturbance will be occur in the injection zone.

In case 8 the obstacle is closer to the injection zone by 15 m for the same conditions of case 6. **Fig. (13)** shows a disturbance in the region of injection because of the imminence of the obstacle and after the disturbance region the stream lines are steady in the longitudinal direction.

When the obstacle is far away from the injection zone by 15 m (case 9) there is no effect on the stream lines as shown in **Fig. (14)**.

The velocity vector

The flow field can be demonstrated in a vector form to show the value and direction of the velocities in the river area for the 9 cases. **Figures (15) and (16)** show the velocity vector for a river without and with obstacle respectively and without injection for both cases. It is clear from **Fig. (16)** that the velocity vector is disturbed near the obstacle.

When the obstacle exist with the injection as in case 3 the velocity decrease near the injection zone as shown in **Fig. (17)** Compared with that in **Fig. (18)** for case 4 because of the existing of the obstacle

Fig. (18) for case 4 shows that the higher velocity vector is near the injection zone and its value reduced away from the injection zone.

The velocity vector increase higher near the injection zone in case 5, compared with that in case 4 because of the increase in injection velocity and this are clear in **Fig. (19)** while in **Fig. (20)** the velocity vectors are seen to be decrease and become very small near the obstacle.

In **Fig. (21)** the obstacle is closer to the injection zone which noted a shifting occurred near the injection zone compared with that in **Fig. (22)** for isle far away from the injection zone.

Temperature Field

The temperature field was obtained by the numerical solution of the energy equation for the 8 cases in configuration considered in the previous section. The net local energy rejected from each finite element of the surface of the river as a function of the finite element local surface temperature, turbulent flow (k-ε) model, incompressible fluid, different injection temperature, different injection velocity and different obstacle location (closer or farness) in river.

The results of the temperature field are clear in **Fig. (23)** and **Fig. (24)** for case 3 and case 4 which show the temperature distribution in the river region of 1000 m length and 150 m width. The injection temperature for the two cases is $T_{inj} = 298^\circ \text{K}$ and a decrease in temperature of hot water injected and the isotherms are seen to be clustered around the injection zone then the temperature decays in all directions away from injection towards river due to the convection heat transfer as net energy lost from the river to the environment. The isotherms obtained by (Seghal and Jaluria 1982) are qualitatively similar to the isotherms obtained in this work. Comparing **Fig. (23)** and **Fig. (24)** Shows similarity due to the grate area providing bigger region of dissipating a large amount of heat transfer to the environment and obtaining lower temperature far away from injection zone.

Fig. (25) and **Fig. (26)** With grater injection velocity for cases 5 and 6 without and with obstacle respectively are shown the isotherms obtained to be clustered around the injection and to have increasing value when moving away from the injection opening toward river. The shape of the contours differs from that in **Fig. (23)** and **(24)**. It is clear that the temperature is taken wider region due to the increase in injection velocity. Comparing **Fig. (25)** and **Fig. (26)** it is clear that there is different distance of temperature distribution or wide region of temperature distribution for the case with obstacle in the river, so the obstacle is an obstacle disturbs the temperature distribution and after this obstacle the temperature distribution will be steady.

The isotherms profiles with injection are shown in **Fig. (26)** with $T_{inj} = 298^\circ \text{K}$ and in **Fig. (27)** with $T_{inj} = 313^\circ \text{K}$ and **Fig. (28)** with $T_{inj} = 318 \text{ k}$. respectively. The three cases have the same condition of isle existing and velocity injection but, the variation between the three figures are very small. So the temperature distribution area increases in the last case.

Fig. (29) shows the isotherms for the river with obstacle closer to injection zone and other conditions are as in case 6 but the difference in temperature distribution region increases due to the decrease of the distance between the obstacle and the injection zone.

It is clear from **Fig. (30)** which is of the same conditions as case 6 but with obstacle existing far away from the injection zone by 15 m that the isotherms of this case is the same as in case 6 because this area is not affected by the farness obstacle.

Comparison with an Actual Case

The estimated weather conditions for cooling ponds are listed below:-

$$U_\infty = 0.1 \text{ m/s}$$

$$\text{length} = 300 \text{ m}$$

$$\text{width} = 10 \text{ m}$$

$$\Delta t = 10 \text{ C}^\circ$$

$$\text{Re}_t = 1000$$

$$\text{Pe}_t = 1000$$

$$T_{in} = 36 \text{ C}^\circ$$

$$T_\infty = 23 \text{ C}^\circ$$



The inflow temperature was taken to be approximately 36 C° . The contour lines close to the inflow both cases (present work and cooling ponds (**Kasim Daws**)) are seen to be clustered around the inflow and a reducing value by moving a way from the inflow opening toward the length river. Selected results and calculations concerning the thermal temperature of the cooling river under study are presented **Fig. (5, 6)** are same cooling ponds (**Kasim Daws**) **Fig. (31, 32)** but the temperature distribution **Fig. (33)** different between the present work **Fig.(34)** because the cooling ponds taken study the following:-

1. Solar heat flux.
2. Evaporation heat-exchange.
3. Heat flux due to back radiation
4. Surface temperature.
5. Weather different.

CONCLUSION

The contour lines close to the inflow in all cases are seen to be clustered around the inflow and reducing value by moving away from the inflow opening toward the long river. From the results of the present work it was concluded that the increase in injection velocity cause a disturb near the injection zone and affect the area of temperature distribution and stream lines and so was the obstacle exist but the in crease injection temperature cause a small effect. The closer obstacle to the injection zone by 15m cause more disturbances in this area.

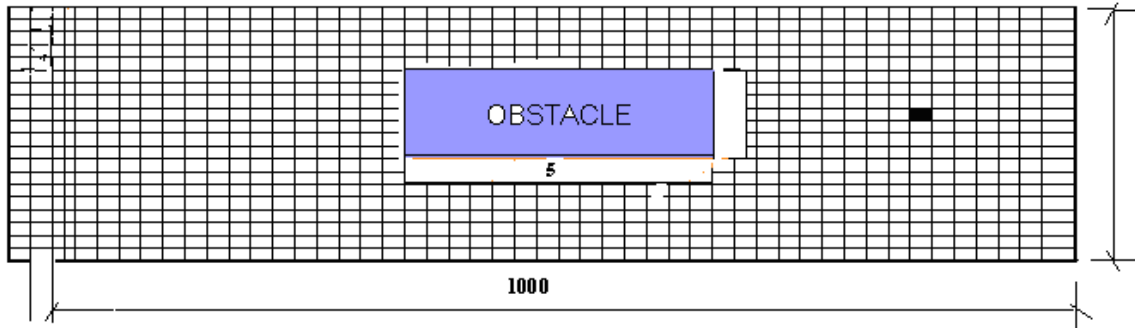


Fig.1: The Problem of the Present Work

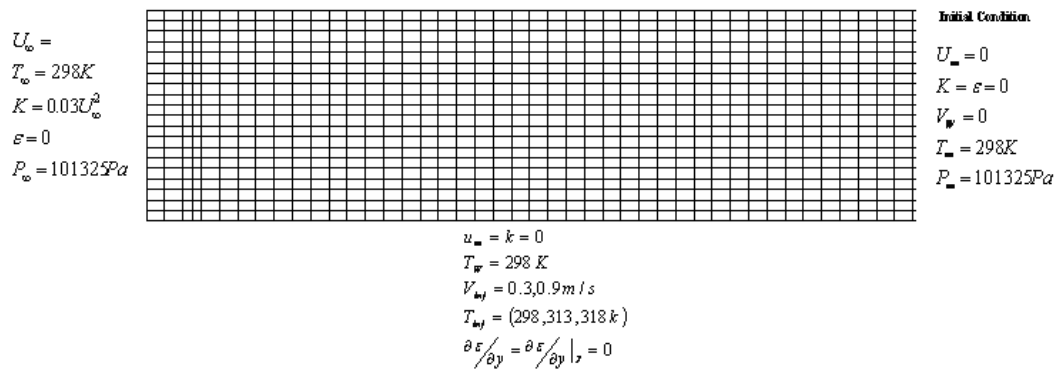


Fig.2: The Initial and Boundary Condition

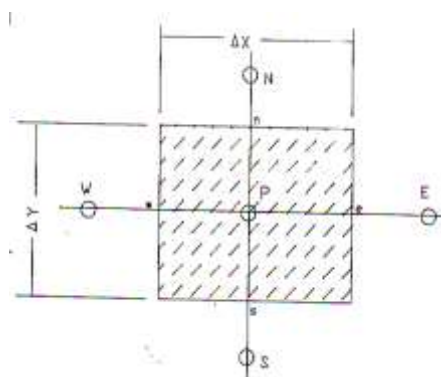




Fig.3: The Volume for Tow-Dimensional Case

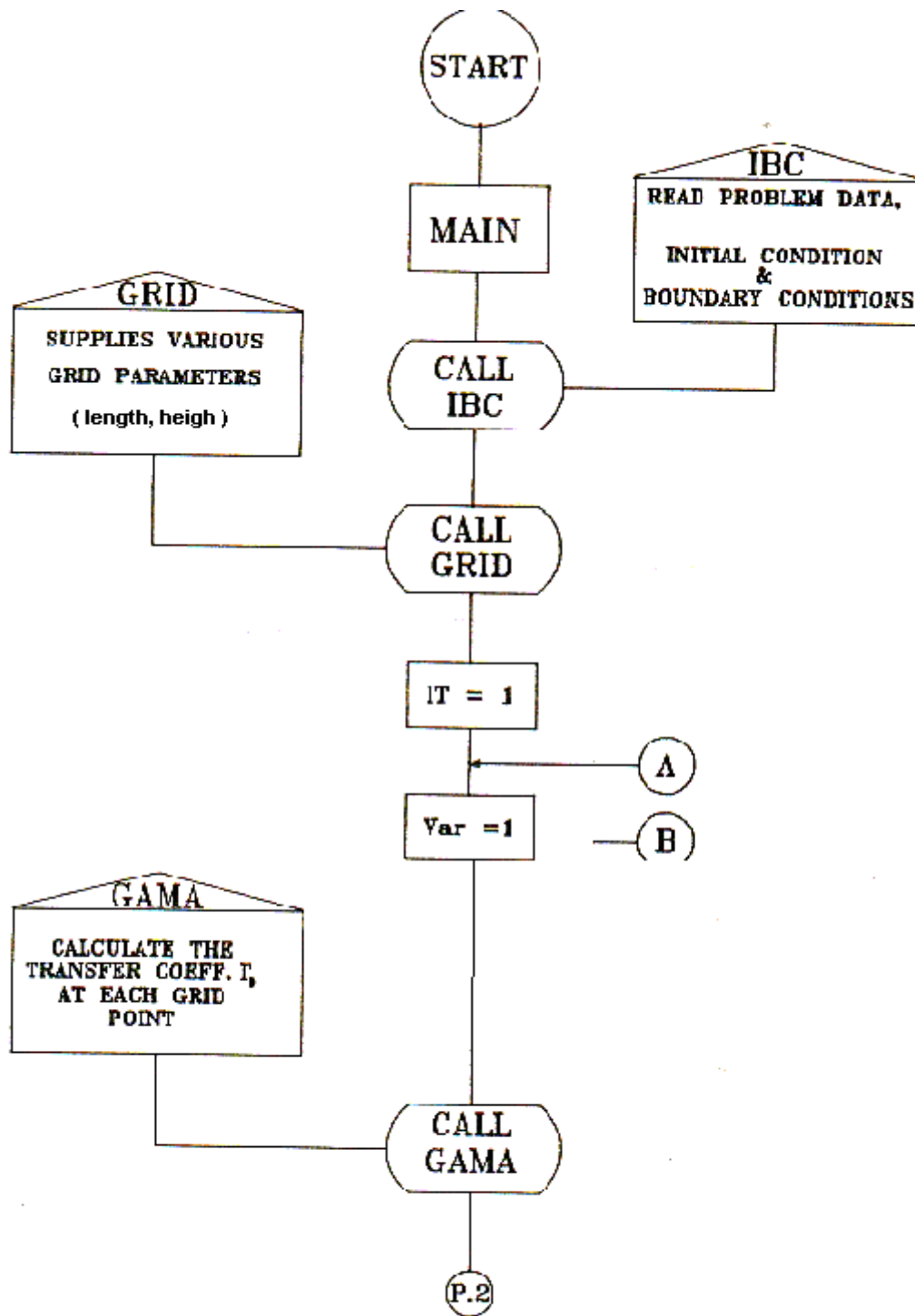
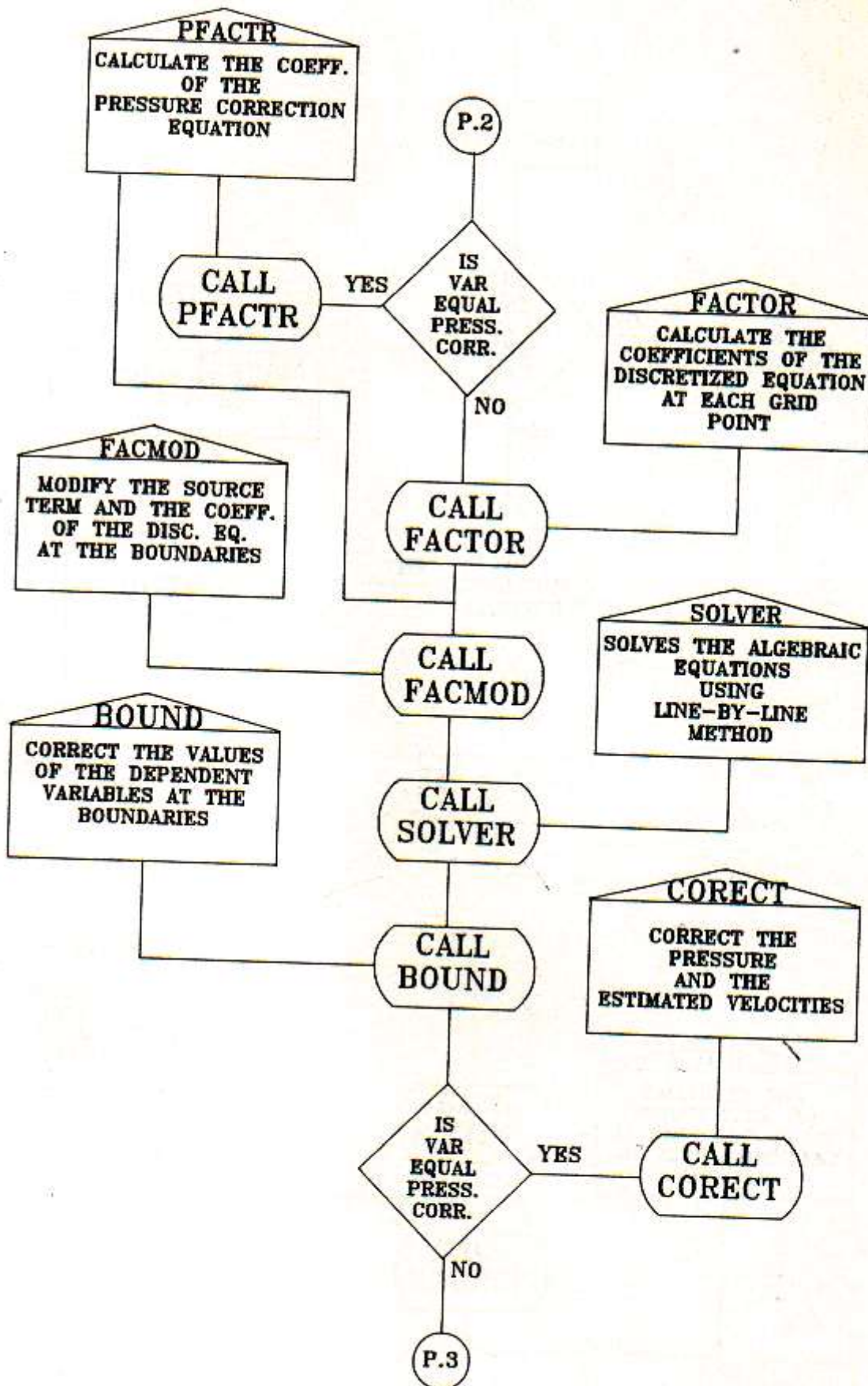


Fig.4: Flow Chart for the Numerical Model



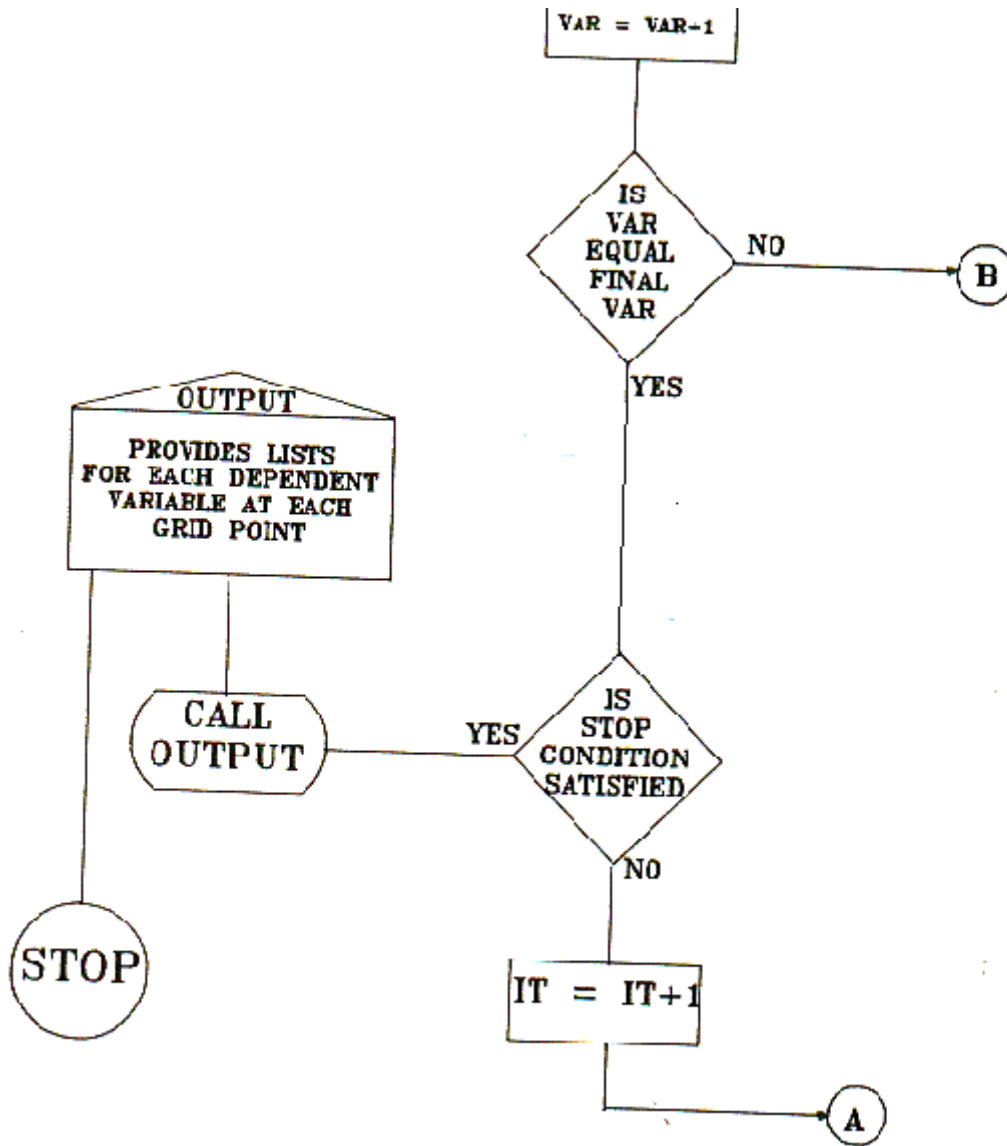




Fig. 5: Stream Lines for case 1

STREAM LINES
KEY TO CONTOUR VALUES
A 1.406E+05
B 1.219E+05
C 1.031E+05
D 8.438E+04
E 6.563E+04
F 4.688E+04
G 2.813E+04
H 9.375E+03

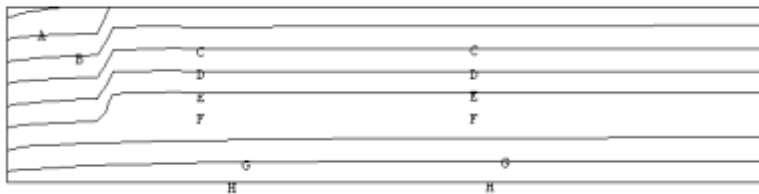


Fig. 6: Stream Lines for case 2

STREAM LINES
KEY TO CONTOUR VALUES
A 1.406E+05
B 1.219E+05
C 1.031E+05
D 8.438E+04
E 6.563E+04
F 4.688E+04
G 2.813E+04
H 9.375E+03

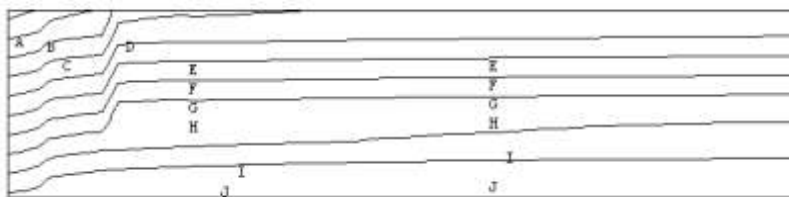


Fig. 7: Stream Lines for case 3

STREAM LINES
KEY TO CONTOUR VALUES
A 1.423E+05
B 1.270E+05
C 1.117E+05
D 9.635E+04
E 8.102E+04
F 6.569E+04
G 5.036E+04
H 3.503E+04
I 1.970E+04
J 4.365E+03

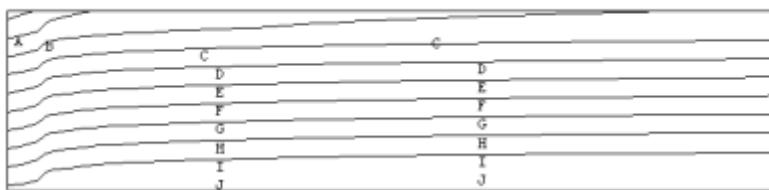
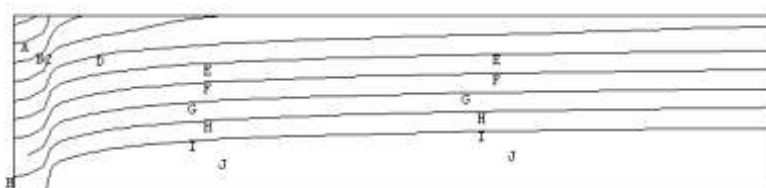


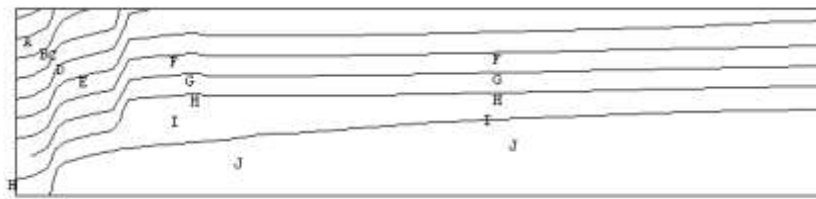
Fig. 8: Stream Lines for case 4

STREAM LINES
KEY TO CONTOUR VALUES
A 1.423E+05
B 1.270E+05
C 1.117E+05
D 9.635E+04
E 8.102E+04
F 6.569E+04
G 5.036E+04
H 3.503E+04
I 1.970E+04
J 4.365E+03



STREAM LINES
KEY TO CONTOUR VALUES
A 1.420E+05
B 1.260E+05
C 1.100E+05
D 9.400E+04
E 7.800E+04
F 6.200E+04
G 4.600E+04
H 3.000E+04
I 1.400E+04
J -2.000E+03

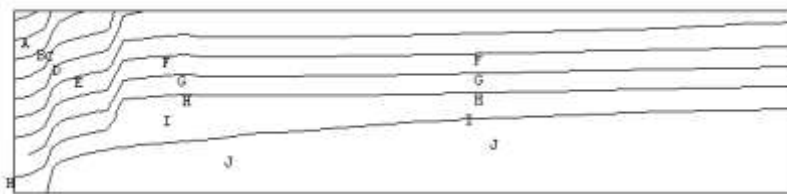
Fig. 9: Stream Lines for case 5



STREAM LINES
KEY TO CONTOUR VALUES

A	1.420E+05
B	1.260E+05
C	1.100E+05
D	9.400E+04
E	7.800E+04
F	6.200E+04
G	4.600E+04
H	3.000E+04
I	1.400E+04
J	-2.000E+03

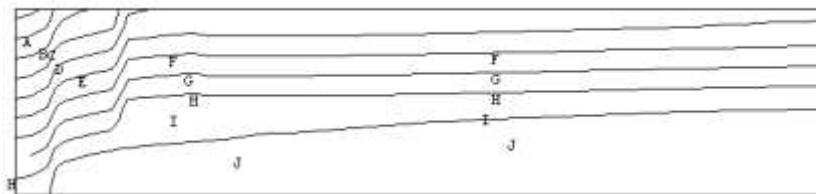
Fig. 10: Stream Lines for case 6



STREAM LINES
KEY TO CONTOUR VALUES

A	1.420E+05
B	1.260E+05
C	1.100E+05
D	9.400E+04
E	7.800E+04
F	6.200E+04
G	4.600E+04
H	3.000E+04
I	1.400E+04
J	-2.000E+03

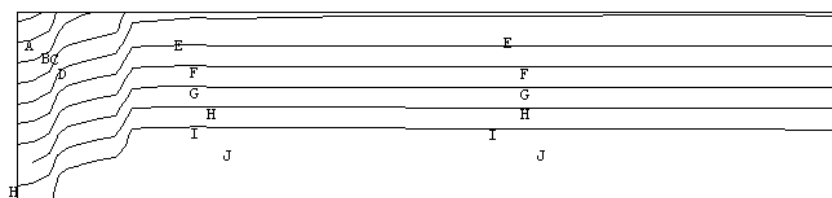
Fig. 11: Stream Lines for case 7



STREAM LINES
KEY TO CONTOUR VALUES

A	1.420E+05
B	1.260E+05
C	1.100E+05
D	9.400E+04
E	7.800E+04
F	6.200E+04
G	4.600E+04
H	3.000E+04
I	1.400E+04
J	-2.000E+03

Fig. 12: Stream Lines for case 8



STREAM LINES
KEY TO CONTOUR VALUES

A	1.420E+05
B	1.260E+05
C	1.100E+05
D	9.400E+04
E	7.800E+04
F	6.200E+04
G	4.600E+04
H	3.000E+04
I	1.400E+04
J	-2.000E+03

Fig. 13: Stream Lines for case 9

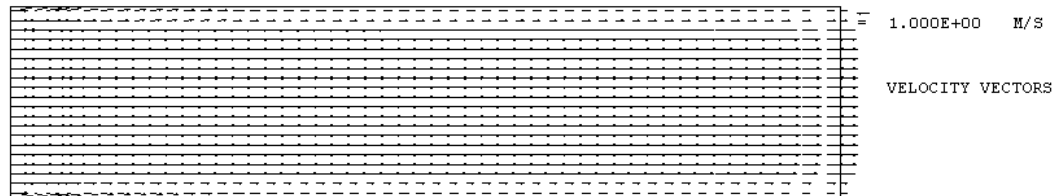
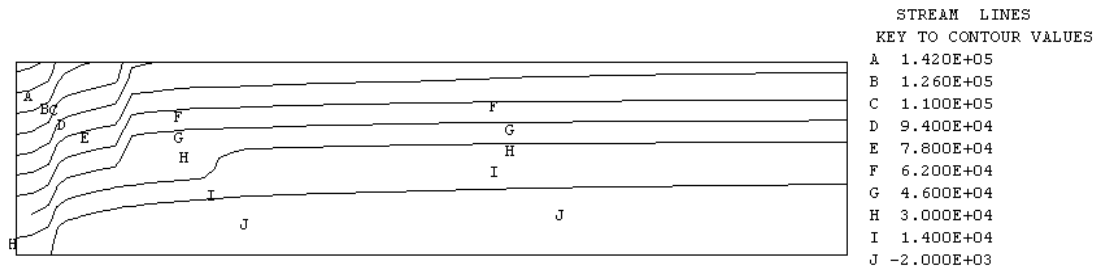


Fig. 14: Stream Lines for case 10
ig. 15: velocity Vectors for case1

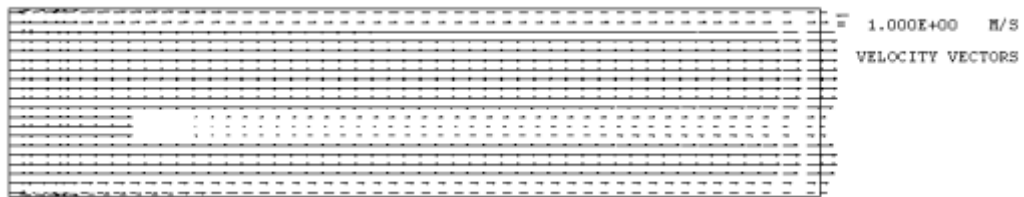


Fig. 16: Velocity Vectors for case2

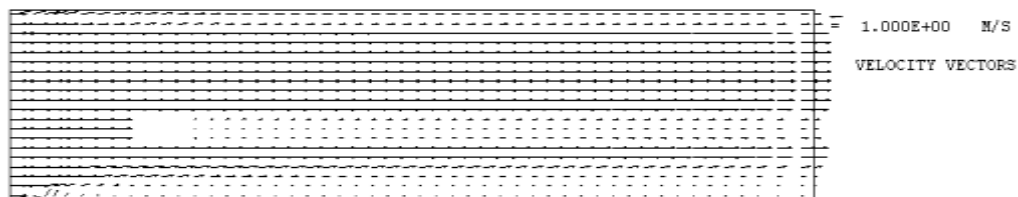


Fig. 17: Velocity Vectors for case3

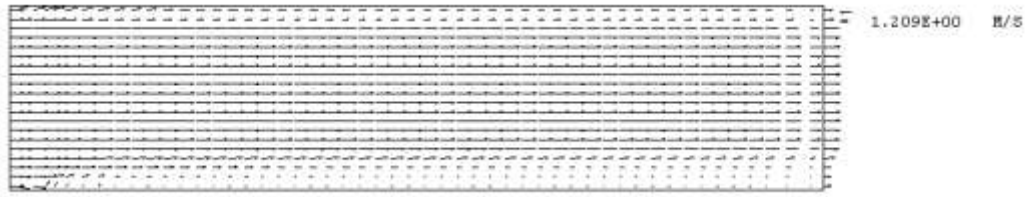


Fig. 18: Velocity Vectors for case4

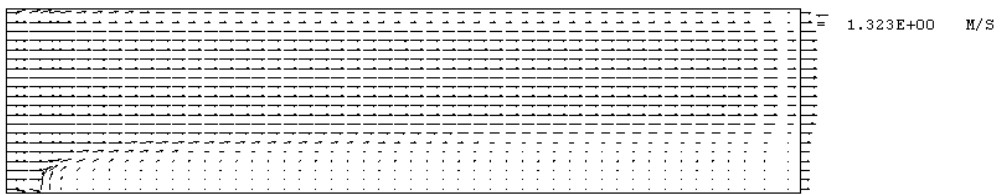


Fig. 19: Velocity Vectors for case5

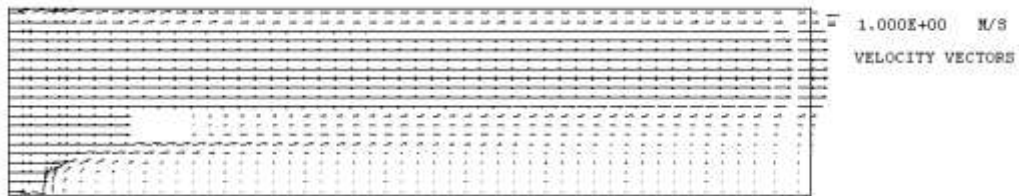


Fig. 20: Velocity Vectors for case6

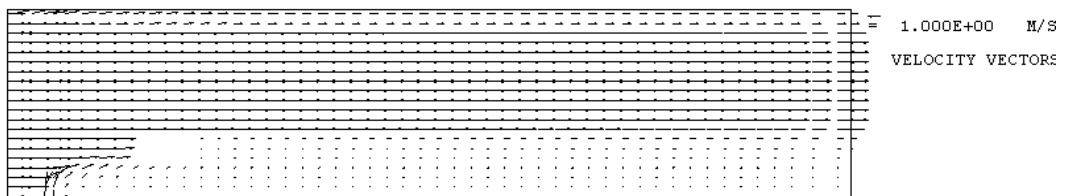


Fig. 21: Velocity Vectors for case9

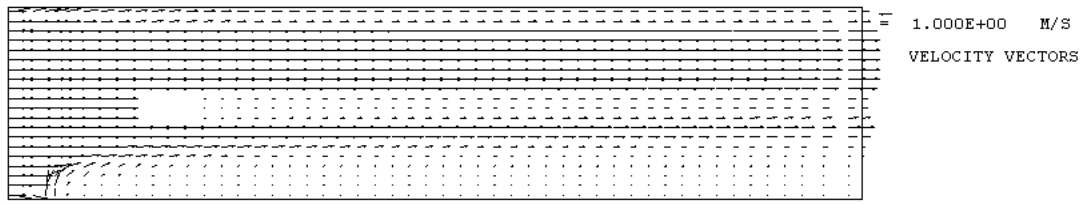


Fig. 22: Velocity Vectors for case10

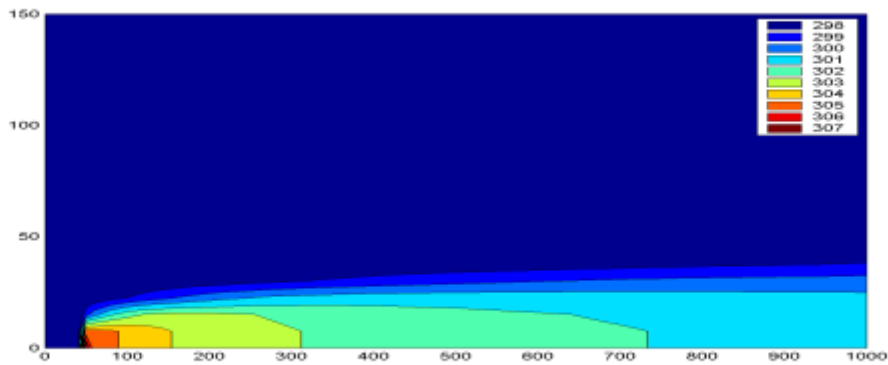


Fig.23: Isotherms for case3

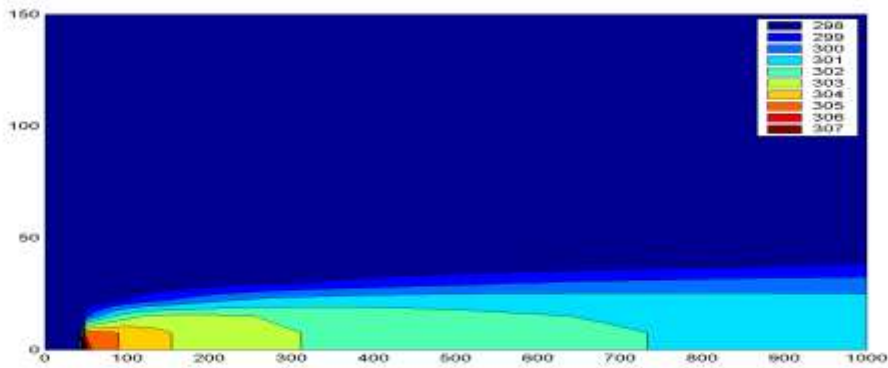


Fig.24: Isotherms for case4

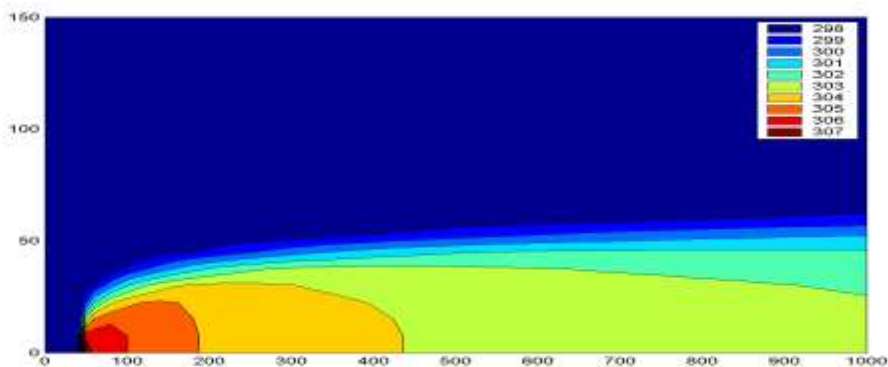


Fig.25: Isotherms for case5

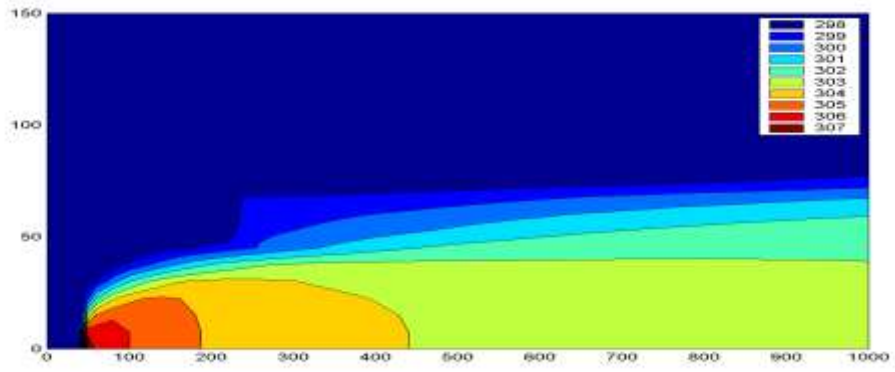


Fig.26: Isotherms for case6

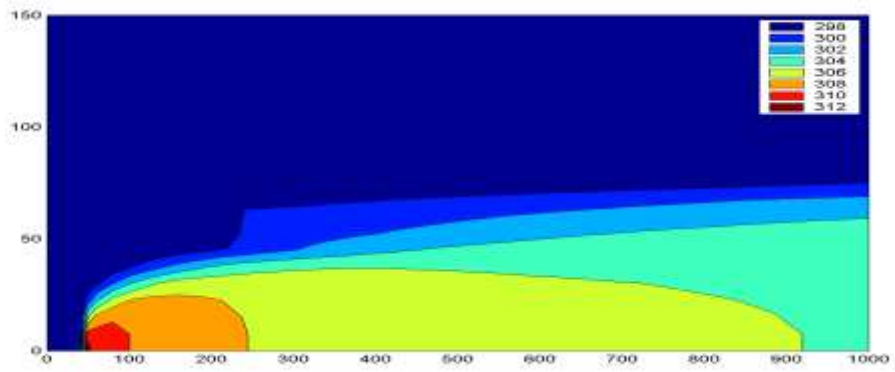


Fig.27: Isotherms for case7

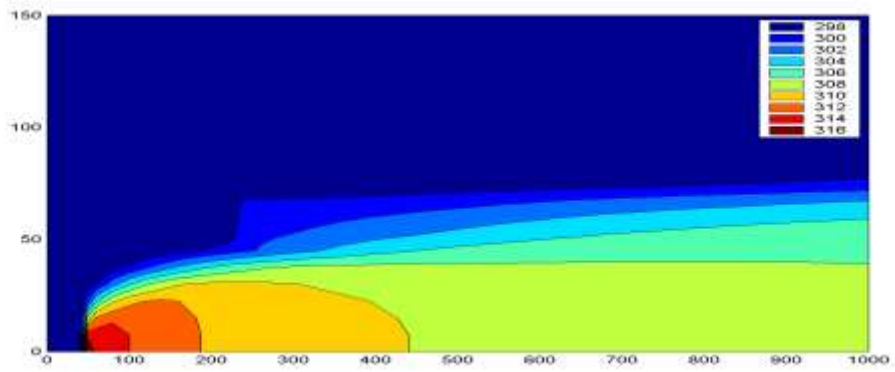


Fig.28: Isotherms for case8

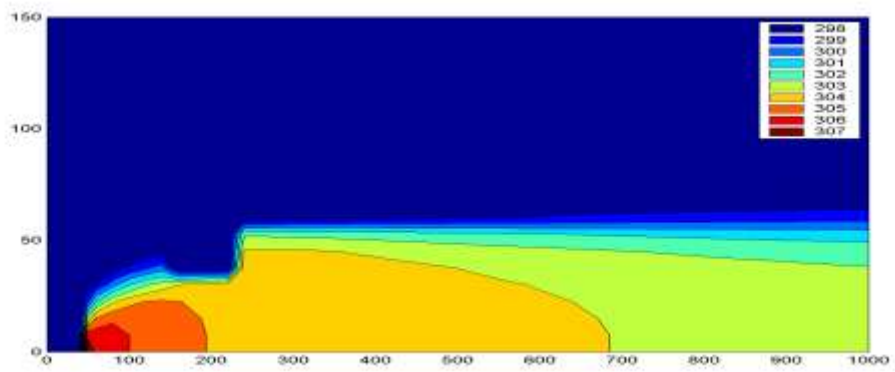


Fig.29: Isotherms for case9

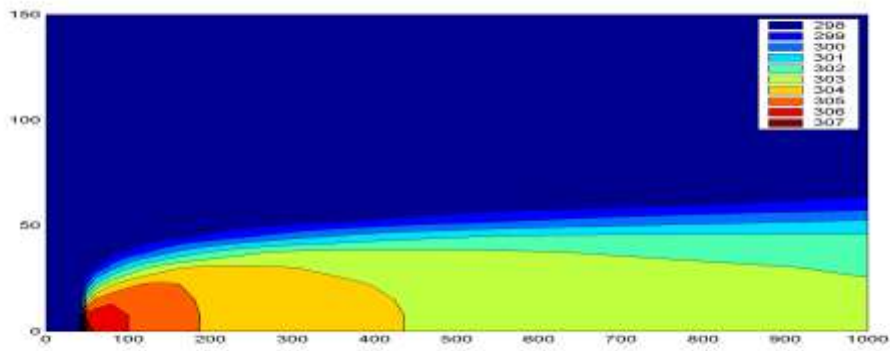


Fig.30: Isotherms for case10

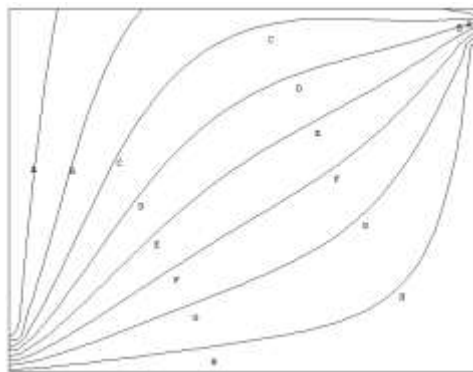


Fig. 31: Stream Lines for same (present work and cooling ponds)

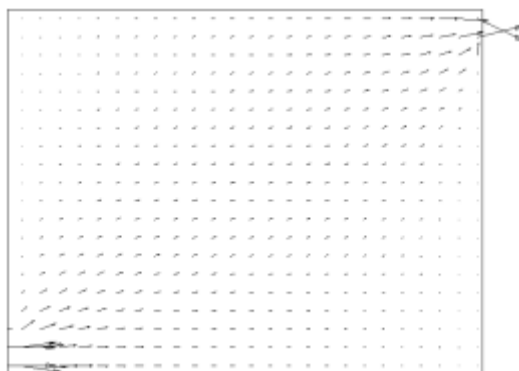


Fig. 32: Velocity Vectors for same (present work and cooling ponds)

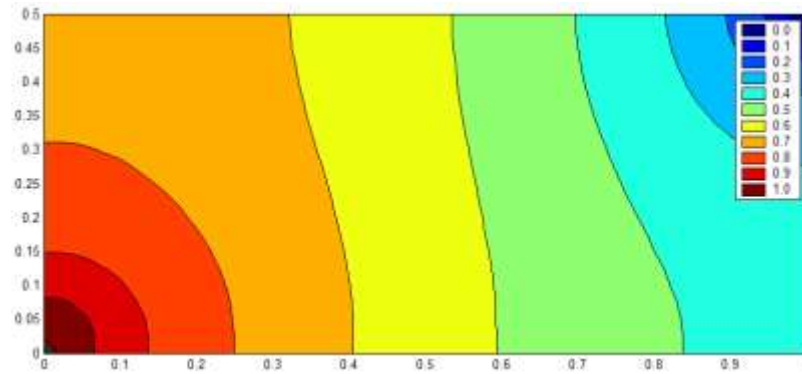


Fig.33: Isotherms for cooling ponds

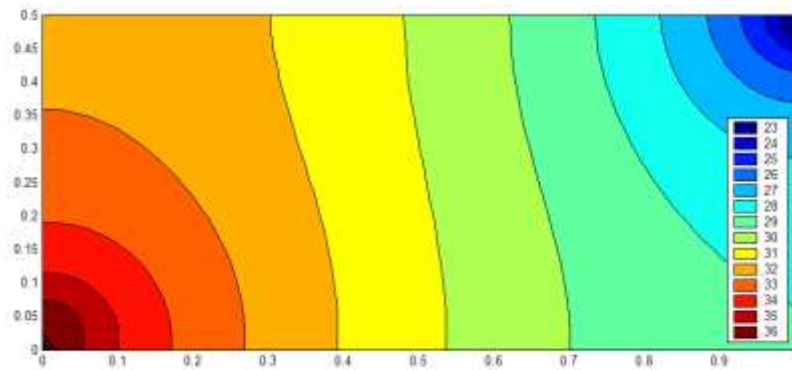


Fig.34: Isotherms for present work

REFERENCES

- Andrzej Pozlewicz" Modeling of thermal pollution dispersion in lower Odra river" Department of Geotechnical Engineering, Szczecin University of Technology, Poland, al. Piastow 50, PL 70-311 Szczecin, Poland.
- ASCE Task Committee on Turbulence Model in Hydraulic Computation "Turbulence Modeling of surface water Flow and Transports part I", Journal of Hydraulic Engineering Vol. 114, No9, sep. (1988).
- A.Zukauskas"Warm-watre spreading in cooling ponds of steam power plants" Heat transfer and turbulent buoyant convection, vol.1, pp.139, (1976).
- H.Inhaber,water encyclopedia,vol.1, wiley-interscience,pp.560-565(2005).
- International atomic energy, thermal discharge at nuclear power station, their management and environmental impacts. Technical report series 155.1974.
- Kasim Daws"Heat Exchange and Dissipation in Large Water Bodies",M.Sc. Thesis, Mech.,Eng., Dept., University of Baghdad, 1990.
- M. Anis AL-Layla and Hasan AL-Rizzo" Awater quality model for the Tigris River downstream of Al Mosul Dam, Iraq"Hydrological Sciences, Vol.34, No.1, June, PP. 687, (1990).
- Michael Manga and James W.Kirchner"Interpreting the temperature of water at cold springs and the importance of gravitational potential energy' Water Resources Research, Vol.40, W05110, doi: 10.1029/2003WR002905, 2004.



- Ministry of health directorate genera of human environment the limits of the regulation of rivers and public waters from the pollution No.25 for a year (1967).

-M. J. Joyce and S. N. Port, Environmental Impact of Power Generation, 11, Issues in Environmental Science and Technology, Royal Society of Chemistry(1999).

- Nagano Y. and Hishida M., "An Improved $\kappa - \varepsilon$ Model for Boundary Layer Flows " J. Fluid Mech., vol. 112, PP. 33-39, March (1990).

- Patanker S.V. "Numerical Heat Transfer and Fluid Flow", Mc Graw-Hill Book Company, N.Y., (1980).

- R.C. Sehgal and Y. Jaluria"Horizontal Recirculation in Water Bodies due to Thermal Discharge" Energy, vol.7, No.5, PP. 419-428, 1982.

NOMENCLATURE

C_p	The Specific heat at Constant Pressure, (=1004.5 J/kg.K)	
F	Convective Flux Through a cell Face	m^2/sec
K	Thermal Conductivity	W/m. K
k	Kinetic Energy of Turbulence	J
K	Ratio of Specific's Heat, (=1.4 for air)	
P	Pressure	N/m^2
P	Cell Nodal Point	
Re	Reynolds Number	
T	Temperature	K
T_w	the Wall Temperature	K
t	Time	sec
U	The Velocity Vector	m/sec
u, v, w	Velocity Components in the x, y and z	m/sec
X, x	X-Coordinate Distance	m
Y, y	Y-Coordinate Distance	m

Greek letters

ε	Dissipation Rate of Turbulent	
$\Delta X, \Delta Y, \Delta Z$	Cell Distances	
$\partial k, \partial \varepsilon$	Constant in the $K - \varepsilon$ Model	
$\partial x, \partial y$	Half the Cell Distances	
Φ	Dependent Variable in the General Form of Equation	
Γ	Transfer Coefficient	
μ	Laminar Viscosity	kg/m.s
μ_{eff}	Effective Eddy Viscosity	kg/m.s
μ_t	Turbulent Viscosity	kg/m.s
ρ	Density	kg/m^3
ν	Kinematics Viscosity	m^2/s
τ_w	Wall Shear Stress	N/m^2

Subscripts

e, w, n, s	(east, west, north, south) nodes at the cell face
l	Laminar
o	Initial Value
t	Turbulent
u, v, w	Velocity Component in x, y, and z directions
1, 2, 3	Coordinate Direction

Superscripts

t	Turbulent
$*$	Predicted Values
$,$	Fluctuation Values, Correction Values
∞	Signifies Free Stream Conditions

Abbreviations

F.D.M	Finite Difference Method
SIMPLE	Semi-Implicit Method for pressure-Linked Equation